Selection of controlled variables: A novel perspective based on the singular energy of weighted graphs

David Zumoffen [*,1], Estanislao Musulin [2]

Computer Aided for Process Engineering Group (CAPEG), French-Argentine International Center for Information and Systems Sciences (CIFASIS-CONICET-UNR-AMU), 27 de Febrero 210 bis, S2000EZP Rosario, Argentina

ARTICLE INFO

ABSTRACT

The optimal selection of controlled variables is a well-known plant-wide control subproblem. In this paper, a novel approach based on spectral graph theory is proposed. This strategy is useful from both graphical and mathematical point of views. It is shown here that if the closed-loop process is represented by a specific weighted graph, deviations in plant variables are bounded by the graph singular energy. Moreover, this graph-based methodology supports the fast interpretation of the magnitude and direction of influences between process variables at steady state. The suggested spectral approach is compared with the recently proposed minimum square deviation (MSD) methodology in detail. Indeed, both strategies have strong structural and behavioral resemblances, i.e. reducing specific deviations and improving the conditions of the subprocess to be controlled. The introduced graph representation is tested in the Shell oil fractionator process, giving a complete set of evaluations and results.

© 2013 Elsevier Ltd. All rights reserved.

1. Introduction

Modern industrial processes are complex and highly interconnected; process plants operation is limited by environmental, economical and operational restrictions. As a consequence, they require the definition and implementation of proper control policies to attain the desired operation performance, maintaining stability and minimizing the effects of unmeasured disturbances.

The plant-wide control (PWC) area addresses the above stated problem from a global perspective. Some of the objectives of PWC are the optimal selection of controlled and manipulated variables (CVs and MVs), the input–output variable pairing, the controller structure (decentralized or centralized) and tuning. Most of these decisions are combinatorial problems in nature, which generally are solved by using heuristic concepts as well as engineering knowledge. While the processes dimension (i.e. amount of inputs and outputs) increases this heuristic treatment becomes quickly impractical, and the problem is frequently reduced ad-hoc generating suboptimal solutions. In this context, a systematic and generalized tool for PWC design is very helpful.

There are several approaches for dealing with the PWC problem, most of them based on process control and system analysis theories (Khaki-Sedigh & Moaveni, 2009; Skogestad & Postlethwaite, 2005). These methodologies range from simple steady-state analysis to complex frequency-based optimization routines. The systematics, generalization, and efficiency of such strategies are varied. The development of scalar indexes are welcomed by process and control engineers because they promote their use into optimization algorithms which systematize and generalize the PWC problems. An example of such methodologies is the recently appeared minimum square deviation (MSD) approach (Molina, Zumoffen, & Basualdo, 2011; Zumoffen & Basualdo, 2012, 2013). MSD uses the sum of square deviations (SSD) and the net load evaluation (NLE) indexes to quantify several steady-state deviations of the process variables at closed-loop. These indexes are integrated into combinatorial problems and multi-objective binary optimization algorithms to evaluate the multivariate process interaction caused by changes on set points and disturbances.

In this work a new perspective for representing and solving some PWC subproblems is presented. The motivation here, relies on the general idea of unifying the process information management (control, modeling, monitoring) via spectral graph theory. Due to the graphical potential and the well-defined mathematical background of this theory, the classical control/process engineers' tasks could be improved with suitable information (quantity and quality). In this context, the work proposed here, summarizes interesting preliminary results related to the first step the PWC, addressed from the spectral graph point of view. It is shown that some PWC subtasks such as the optimal CVs selection can be

---

* Corresponding author. Tel.: +54 0341 4237248x332; fax: +54 0341 482 1772.
  E-mail addresses: zumoffen@cifasis-conicet.gov.ar (D. Zumoffen),
musulin@cifasis-conicet.gov.ar (E. Musulin).
  [1] Address: Universidad Tecnológica Nacional – FRRo, Zeballos 1341, S2000BQA, Rosario, Argentina.
  [2] Address: Universidad Nacional de Rosario – FCEyA, Pellegrini 250, S2000BTP, Rosario, Argentina.

Nomenclature

Acronyms

CVs	controlled variables
DVs	disturbances variables
IMC	internal model control
MSD	minimum squared deviation
MTF	matrix of transfer functions
MVs	manipulated variables
NLE	net load evaluation
PWC	plant-wide control
SSD	sum of squared deviations
UVs	uncontrolled variables

Variables

$\mathbf{A}$	adjacency matrix
$\mathbf{A}_w$	weighted adjacency matrix
$\mathbf{A}_w^{cl}$	weighted adjacency matrix – closed-loop
$\mathbf{d}(s)$	disturbance vector
$\mathbb{E}(G)$	energy of graph G
$\mathbb{E}_s(G)$	singular energy of graph G
$\mathbf{e}(i)$	vector with unitary entry in the ith location
$\mathbf{D}(s)$	disturbance MTF
$\mathbf{D}_r(s)$	disturbance MTF for UVs
$\mathbf{D}_s(s)$	disturbance MTF for CVs
$\mathbf{F}(s)$	diagonal low pass MTF filter
$G(V, E)$	undirected weighted graph
$\mathbf{G}(s)$	process MTF
$\mathbf{G}_c(s)$	controller MTF
$\mathbf{G}_r(s)$	process MTF for UVs
$\mathbf{G}_r(s)$	process MTF for CVs
$\tilde{\mathbf{G}}_s(s)$	process model MTF for CVs
m	number of outputs
n	number of inputs
p	number of disturbances
s	Laplace variable
$SSD(\mathbf{a})$	sum of squared deviations of $\mathbf{a}$
t	time
$\mathbf{u}(s)$	input vector
$\mathbf{y}(s)$	output vector
$\mathbf{y}_r(s)$	UVs vector
$\mathbf{y}_s(s)$	CVs vector
$\mathbf{y}_s^{sp}(s)$	set point vector

Greek symbols

γ	condition number
λ_i	ith eigen value
σ_i	ith singular value
$\underline{\sigma}$	minimum singular value
$\overline{\sigma}$	maximum singular value

efficiently solved by analyzing the spectral properties of a properly defined weighted graph. Before going into further details, let us introduce some general graph concepts.

Many real-world situations can conveniently be represented by a diagram consisting of a set of vertices joined by a set of edges. For example, vertices could be people, communication centers or process variables, and the corresponding edges could represent friendship links, communications links and interactions degree, respectively. A mathematical abstraction of these situations led to the concept of graph (Bondy & Murty, 1985). A graph can be represented by its adjacency matrix $\mathbf{A}$; the analysis of $\mathbf{A}$ based on eigen values, eigen vectors, singular values and energy (Gutman & Shao, 2011; Nikiforov, 2007) is called the theory of graph spectra. This

theory attempts to utilize linear algebra including, in particular, the well-developed theory of matrices, for purposes of graph theory and its applications (Cvetković, Rowlinson, & Simić, 2010).

Spectral graph theory has acquired great relevance in the last decade, particularly in the computer science area. An excellent survey of these applications can be found in Cvetković and Simić (2011). Other research areas such as process engineering have very few applications of this spectral approach. Anyway, there are some works related to graph theory such as Castaño Arranz and Birk (2012) where new methods for the analysis of complex processes are suggested. The authors formulated a flexible framework to help the designers in comprehending a process by representing structural and functional relationships. Yang, Shah, and Xiao (2012) suggested a fusion of information from process data and process connectivity. Signed directed graphs are used to capture the process topology and connectivity, thus depicting the causal relationships between process variables. Gutierrez-Perez, Herrera, Perez-Garcia, and Ramos-Martinez (2011) introduced a methodology based on spectral measurements of graphs to establish the relative importance of areas in water supply networks. These areas are analyzed using a flexible method of semi-supervised clustering.

Here, we present a methodology to optimally select CVs based on the singular energy of a graph. We found that if the closed-loop process is represented by a weighted graph, its energy (based on its adjacency matrix $\mathbf{A}$) is strongly related to deviations in some plant variables. Moreover, the singular energy is an upper bound for the interaction effects between all the vertices of the weighted graph in a SSD sense (Frobenius norm). Explicitly, it is show that the SSD concept applied to the overall graph structure is equivalent to quantify the deviations in the vertices corresponding to MVs and uncontrolled variables (UVs) only.

This result shows a clear structural resemblance with the approach called MSD-SSD presented by Zumoffen and Basualdo (2012, 2013), but in this case from a spectral graph point of view. Hence, the optimal CVs selection can be performed by minimizing the singular energy of the graph. Furthermore, the analysis shows that this minimization has similar properties to those obtained using the SSD approach. Particularly, both methodologies tend to improve the matrix-properties of the subprocess to be controlled (i.e. tend to maximize their minimum singular value). This is an important quality, strongly related to the final closed-loop behavior, as stated by (Garcia & Morari, 1985; Grosdidier, Morari, & Holt, 1985; Skogetad & Morari, 1987).

The work is organized as follows. Section 2 gives a background on some already existing tools and methodologies. Section 2.1 presents a simplified description of the MSD approach suggested by Zumoffen and Basualdo (2012, 2013). In particular, the optimal CVs subproblem is described. In Section 2.2 the main graphs concepts used in this work are defined. The most important contribution of this paper is introduced in Section 3, where the main links between the classical SSD and the singular energy-based approaches are highlighted. Both methodologies are applied to the well-known Shell oil fractionator process in Section 4, where several simulation results are presented. Conclusions and future work are discussed in Section 5.

2. Background and tools

2.1. Minimum square deviation

The minimum square deviation (MSD) approach suggested by Zumoffen and Basualdo (2012, 2013) addresses several PWC tasks such as: the optimal selection of CVs and MVs, the input–output pairing, the controller interaction degree (decentralized, full or sparse), and the controller oversizing analysis (order). In this case, for clarity, only a simplified version of the MSD methodology is considered.
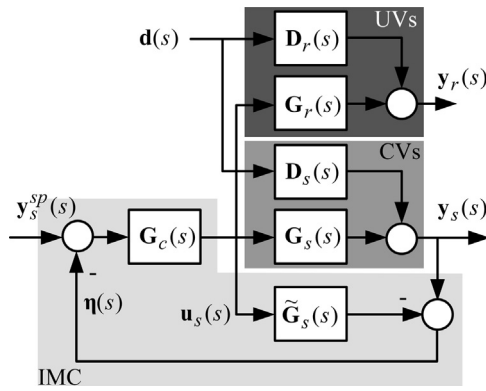
Fig. 1. IMC structure.

Let us consider an industrial process with m potential CVs, n available MVs, p disturbances (DVs), and assume that $m > n$. The main PWC objective is to select the optimal n CVs from a total of m, thus squaring-down the overall control problem.

The model of the process can be represented and partitioned by several matrices of transfer functions (MTF) in the Laplace domain as shown in Eq. (1),

$$\mathbf{y}(s) = \mathbf{G}(s)\mathbf{u}(s) + \mathbf{D}(s)\mathbf{d}(s) = \begin{bmatrix} \mathbf{y}_s(s) \\ \mathbf{y}_r(s) \end{bmatrix} = \begin{bmatrix} \mathbf{G}_s(s) \\ \mathbf{G}_r(s) \end{bmatrix} \mathbf{u}(s) + \begin{bmatrix} \mathbf{D}_s(s) \\ \mathbf{D}_r(s) \end{bmatrix} \mathbf{d}(s) \qquad (1)$$

where $\mathbf{y}(s)$, $\mathbf{u}(s)$, and $\mathbf{d}(s)$ are the potential CVs, the available MVs, and the disturbance vectors with dimensions $m \times 1$, $n \times 1$, and $p \times 1$, respectively. On the other hand, the subvectors and submatrices displayed in Eq. (1) have the following representation and description,

$$\mathbf{y}_s(s) = \left[y_s^1(s), \ldots, y_s^n(s) \right]', \qquad \mathbf{y}_r(s) = \left[y_r^1(s), \ldots, y_s^{m-n}(s) \right]'$$

$$\mathbf{G}_s(s) = \begin{bmatrix} g_s^{11}(s) & \cdots & g_s^{1n}(s) \\ \vdots & \ddots & \vdots \\ g_s^{n1}(s) & \cdots & g_s^{nn}(s) \end{bmatrix}, \quad \mathbf{G}_r(s) = \begin{bmatrix} g_r^{11}(s) & \cdots & g_r^{1n}(s) \\ \vdots & \ddots & \vdots \\ g_r^{(m-n)1}(s) & \cdots & g_r^{(m-n)n}(s) \end{bmatrix}$$

$$\mathbf{D}_s(s) = \begin{bmatrix} d^{11}(s) & \cdots & d^{1p}(s) \\ \vdots & \ddots & \vdots \\ d^{n1}(s) & \cdots & d^{np}(s) \end{bmatrix}, \quad \mathbf{D}_r(s) = \begin{bmatrix} d^{11}(s) & \cdots & d^{1p}(s) \\ \vdots & \ddots & \vdots \\ d^{(m-n)1}(s) & \cdots & d^{(m-n)p}(s) \end{bmatrix} \qquad (2)$$

where the output variables has been split in two subsets, being $\mathbf{y}_s(s)$ the n controlled outputs (CVs) and $\mathbf{y}_r(s)$ are the remaining $m - n$ uncontrolled variables (UVs). Moreover, $\mathbf{G}_s(s), \mathbf{G}_r(s), \mathbf{D}_s(s)$, and $\mathbf{D}_r(s)$ are MTF that account for the multivariable effects of MVs and DVs on these subsets. Note that $y_s^i(s)$ is the ith component of the vector $\mathbf{y}_s(s)$ and similarly $g_s^{ij}(s)$ represents the ijth component of the MTF $\mathbf{G}_s(s)$. Since the matrices $\mathbf{G}_r(s), \mathbf{D}_s(s)$, and $\mathbf{D}_r(s)$ are directly determined by $\mathbf{G}_s(s)$, the main objective in this PWC problem (i.e. the selection of controlled variables) can be reduced to the optimal selection of the subprocess $\mathbf{G}_s(s)$.

2.1.1. Considering the control policy

Some insights about the ways to perform the optimal selection of $\mathbf{G}_s(s)$ can be obtained if the control policy is considered. In this case, the Internal Model Control (IMC) theory is used, structured as shown in Fig. 1. This methodology is based on the subprocess model $\tilde{\mathbf{G}}_s(s)$ and the controller design $\mathbf{G}_c(s) = \tilde{\mathbf{G}}_s^{-1}(s)\mathbf{F}(s)$, where $\mathbf{F}(s)$ is a diagonal low-pass filter matrix which guarantees the feasibility of the controller (note that $\mathbf{F}(0) = \mathbf{I}$, where $\mathbf{I}$ is the

identity matrix). Fig. 1 clearly displays the CVs and UVs subgroups, where $\mathbf{y}_s^{sp}(s)$ are the reference trajectories (set points) for the selected CVs.

In the following, the mentioned control structure will be analyzed at steady state ($s = 0$). In the rest of the work the Laplace variable is avoided indicating this fact. If perfect control is assumed $\mathbf{y}_s = \mathbf{y}_s^{sp}$ and there is no plant-model mismatch $\tilde{\mathbf{G}}_s = \mathbf{G}_s$, then the relationships in Eq. (3) hold,

$$\mathbf{u} = \mathbf{G}_s^{-1}\mathbf{y}_s^{sp} - \mathbf{G}_s^{-1}\mathbf{D}_s\mathbf{d}$$

$$\mathbf{y}_r = \mathbf{G}_r\mathbf{G}_s^{-1}\mathbf{y}_s^{sp} + (\mathbf{D}_r - \mathbf{G}_r\mathbf{G}_s^{-1}\mathbf{D}_s)\mathbf{d} = \begin{bmatrix} \mathbf{S}_{sp} & \mathbf{S}_d \end{bmatrix} \begin{bmatrix} \mathbf{y}_s^{sp} & \mathbf{d} \end{bmatrix}' \qquad (3)$$

where $\mathbf{S}_{sp} = \mathbf{G}_r\mathbf{G}_s^{-1}$ and $\mathbf{S}_d = \mathbf{D}_r - \mathbf{G}_r\mathbf{G}_s^{-1}\mathbf{D}_s$ represent the multivariable effects in the UVs given by the set point and disturbance changes, respectively. The severity of these effects depends on the selected control policy parameterized by $\mathbf{G}_s$. Hence, if the process variables are scaled by using the methodology suggested in Skogestad and Postlethwaite (2005) a normalized process model can be obtained. Moreover, a scalar index called sum of square deviations (SSD) can be calculated for quantifying the UVs differences from their normal operating working zone,

$$\text{SSD}(\mathbf{y}_r) = \sum_{i=1}^{n+p} \left|\left| \begin{bmatrix} \mathbf{S}_{sp} & \mathbf{S}_d \end{bmatrix} \mathbf{e}(i) \right|\right|_2^2 = \left|\left| \mathbf{S}_{sp} \right|\right|_F^2 + \left|\left| \mathbf{S}_d \right|\right|_F^2$$

$$= \left|\left| \mathbf{G}_r\mathbf{G}_s^{-1} \right|\right|_F^2 + \left|\left| \mathbf{D}_r - \mathbf{G}_r\mathbf{G}_s^{-1}\mathbf{D}_s \right|\right|_F^2 \qquad (4)$$

where $\mathbf{e}(i)$ is a vector of length $(n + p)$ with an unitary entry in the ith location and zero elsewhere. Note that, $\begin{bmatrix} \mathbf{S}_{sp} & \mathbf{S}_d \end{bmatrix} \mathbf{e}(i)$ are the UVs deviations, from their normal operating point, due to the ith perturbation. On the other hand, $||\mathbf{a}||_2^2 = a_1^2 + \cdots + a_n^2$ and $||\mathbf{A}||_F^2 = \text{tr} \left(\mathbf{A}'\mathbf{A} \right)$ represent the squared Euclidean and Frobenius norms for any vector $\mathbf{a} = [a_1, \ldots, a_n]$ and $(m \times n)$ matrix $\mathbf{A}$, respectively.

Hence, the optimal CVs selection problem can be solved by minimizing the SSD index according to a proper subprocess parametrization for $\mathbf{G}_s$,

$$\min_{\mathbf{G}_s} \text{SSD}(\mathbf{y}_r), \quad \text{subject to } \det(\mathbf{G}_s) \neq 0 \qquad (5)$$

note that condition $\det(\mathbf{G}_s) \neq 0$ guarantees the feasibility of the IMC policy. The combinatorial problem stated in Eq. (5) can be efficiently solved via exhaustive search or some mixed-integer optimization routine depending on the process dimension. In Zumoffen and Basualdo (2010) and Molina et al. (2011) this kind of binary optimization problem was solved via genetic algorithms.

It is worth mentioning that Eq. (4) can be analyzed based on some typical norm and singular value relationships (Bhatia, 1996; Golub & Loan, 1996; Horn & Johnson, 1990; Zhan, 2002). In fact, remembering that for any matrices $\mathbf{A}$, $\mathbf{B}$, and $\mathbf{C}$ with dimension $(m \times n)$, $(n \times m)$, and $(m \times n)$, respectively, we have

$$||\mathbf{A}||_F^2 = \sum_{i=1}^{\min(m,n)} \sigma_i^2(\mathbf{A}), \qquad \overline{\sigma}(\mathbf{A})\underline{\sigma}(\mathbf{B}) \leq \overline{\sigma}(\mathbf{AB}) \leq ||\mathbf{AB}||_F,$$

$$|\overline{\sigma}(\mathbf{A}) - \overline{\sigma}(\mathbf{C})| \leq \overline{\sigma}(\mathbf{A} + \mathbf{C}) \qquad (6)$$

where $\sigma_i(\mathbf{A})$, $\overline{\sigma}(\mathbf{A})$, and $\underline{\sigma}(\mathbf{A})$ are the ith, maximum and minimum singular values of the matrix $\mathbf{A}$, respectively. These expressions allow to obtain the following inequality from Eq. (4),

$$\frac{\underline{\sigma}(\mathbf{G}_r)}{\underline{\sigma}(\mathbf{G}_s)} + |\overline{\sigma}(\mathbf{D}_r) - \overline{\sigma}(\mathbf{G}_r\mathbf{G}_s^{-1}\mathbf{D}_s)| \leq \text{SSD}(\mathbf{y}_r) \qquad (7)$$

which highlights some matrix properties of $\mathbf{G}_s$ when the SSD index evolves. If the $\text{SSD}(\mathbf{y}_r)$ is minimized, then the multivariate effect of references and disturbances on the UVs is reduced at closed

loop. Considering Eq. (7), if the upper bound (right-hand) is minimized, then the left-hand needs to follow this evolution. The main source of singularity in this expression is the minimum singular value $\underline{\sigma}(\mathbf{G}_s)$ or equivalently $\mathbf{G}_s^{-1}$ from Eq. (4). Hence, a SSD($\mathbf{y}_r$) minimization additionally tends to increase $\underline{\sigma}(\mathbf{G}_s)$ in a trade-off solution between $\underline{\sigma}(\mathbf{G}_r)/\underline{\sigma}(\mathbf{G}_s) \to 0$ and $[\overline{\sigma}(\mathbf{D}_r) - \overline{\sigma}(\mathbf{G}_r\mathbf{G}_s^{-1}\mathbf{D}_s)] \to 0$ (Molina et al., 2011; Zumoffen & Basualdo, 2013).

The parameter $\underline{\sigma}(\mathbf{G}_s)$ is an important characteristic of the subprocess to be controlled. In fact, this value is directly related with the well/ill-conditioning of the matrix $\mathbf{G}_s$ and eventually with the closed-loop properties of the control policy. Subprocesses with $\underline{\sigma}(\mathbf{G}_s) \approx 0$ indicates an ill-conditioned and very difficult to control plant. Furthermore, any model-based control policy developed on these kind of processes will have a very low robustness degree (Garcia & Morari, 1985; Grosdidier et al., 1985; Skogetad & Morari, 1987).

2.2. Weighted graphs energy

Let $G = (V, E)$ be a finite undirected weighted graph without loops or multiple edges, and suppose that its vertices are labeled 1, 2, ..., r. If vertices i and j are joined by an edge, we say that i and j are *adjacent* and write $i \sim j$. Since the graph is weighted and undirected, we assume that each edge carries a non-zero symmetric weight ($w_{ij} = w_{ji}$). The elements of the *weighted adjacency matrix* $\mathbf{A}_w$ of the weighted graph G are defined as

$$a_{ij} = \begin{cases} w_{ij} & \text{if } i \sim j \\ 0 & \text{otherwise} \end{cases} \tag{8}$$

Under this definition, $\mathbf{A}_w$ is a real symmetric matrix with zero diagonal. Let $\lambda_1, \ldots, \lambda_n$ be the eigen values of $\mathbf{A}_w$. Then the energy of G is defined as (Gutman, Li, & Zhang, 2009; Gutman & Shao, 2011)

$$\mathbb{E}(G) = \sum_{i=1}^{n} |\lambda_i| \tag{9}$$

This quantity is well known in chemical applications; since in some cases the energy defined in this way corresponds to the energy of a molecule (Cvetković et al., 2010; Gutman, 2005). However, the graph invariant $\mathbb{E}(G)$ can be considered for any graph

independently of the chemical context, recently much work on graph energy appeared also in the "pure" mathematical literature (Gutman & Shao, 2011; Nikiforov, 2007). This new perspective provided new generally valid mathematical properties for $\mathbb{E}(G)$. In this paper is of particular importance the result obtained by Nikiforov (2007), who first recognized that if $\mathbf{A}_w$ is a real symmetric matrix, then the energy of $\mathbf{A}_w$ is the same as the singular energy of $\mathbf{A}_w$, given by

$$\mathbb{E}_s(G) = \sum_{i=1}^{n} \sigma_i(\mathbf{A}_w) \tag{10}$$

where $\sigma_i(\mathbf{A}_w)$ is the ith singular value of $\mathbf{A}_w$, and represents the non-negative square root of the ith eigen value of $\mathbf{A}_w\mathbf{A}_w'$.

3. Controlled variables selection based on weighted graph energy

The graph theory is used here for deriving an alternative representation of this particular PWC problem. In fact, by considering the process representation given in Eq. (1), the steady-state gains from Eq. (2), and the graph concepts stated in Section 2.2, the weighted graph G_{ol} can be developed as shown in Fig. 2 for representing the open-loop plant. In this case, G_{ol} has $(m + 2n + p)$ vertices and $(m \times n + m \times p)$ edges. The n vertices representing the set point variables are unconnected because the control structure is not designed yet. The rest of G_{ol} represents a bipartite graph where there are no interconnection between vertices $u^i - u^j$, $u^i - d_j$, $d_i - d_j$, $y_r^i - y_r^j$, $y_r^i - y_s^j$, and $y_s^i - y_s^j$.

In a similar way, considering the relationships stated in Eqs. (1) and (3), a weighted graph (G_{cl}) can be developed for the process under perfect IMC control as shown in Fig. 3. Note that, G_{cl} is represented in matrix form. Vertices are grouped in "vector vertices" that are represented by black filled circles and connected by weight matrices. For example, the "vector vertex" $\mathbf{y}_s^{sp}$ groups together the single vertices $\{y_{s1}^{sp}, \ldots, y_{sn}^{sp}\}$. As a result, vector vertices $\mathbf{u}$, $\mathbf{d}$, and $\mathbf{y}_r$ have n, p, and $m - n$ components, respectively. Note that there is no direct connection between vertices grouped in a "vector vertex" neither between the vectors vertices $\mathbf{y}_s^{sp}$ and $\mathbf{d}$.

The weighted adjacency matrix $\mathbf{A}_w^{cl}$, for vertices $[y_{s1}^{sp}, \ldots, y_{sn}^{sp}, d_1, \ldots, d_p, u_1, \ldots, u_n, y_r^1, \ldots, y_r^{m-n}]$, results:

$$
\mathbf{A}_w^{cl} = \begin{bmatrix}
0 & \ldots & 0 & 0 & \ldots & 0 & Y^{11} & \ldots & Y^{n1} & 0 & \ldots & 0 \\
\vdots & \ddots & \vdots & \vdots & \ddots & \vdots & \vdots & \ddots & \vdots & \vdots & \ddots & \vdots \\
0 & \ldots & 0 & 0 & \ldots & 0 & Y^{1n} & \ldots & Y^{nn} & 0 & \ldots & 0 \\
0 & \ldots & 0 & 0 & \ldots & 0 & X^{11} & \ldots & X^{n1} & D_r^{11} & \ldots & D_r^{(m-n)1} \\
\vdots & \ddots & \vdots & \vdots & \ddots & \vdots & \vdots & \ddots & \vdots & \vdots & \ddots & \vdots \\
0 & \ldots & 0 & 0 & \ldots & 0 & X^{1n} & \ldots & X^{nn} & D_r^{1p} & \ldots & D_r^{(m-n)p} \\
Y^{11} & \ldots & Y^{1n} & X^{11} & \ldots & X^{1p} & 0 & \ldots & 0 & G_r^{11} & \ldots & G_r^{(m-n)1} \\
\vdots & \ddots & \vdots & \vdots & \ddots & \vdots & \vdots & \ddots & \vdots & \vdots & \ddots & \vdots \\
Y^{n1} & \ldots & Y^{nn} & X^{n1} & \ldots & X^{np} & 0 & \ldots & 0 & G_r^{1n} & \ldots & G_r^{(m-n)n} \\
0 & \ldots & 0 & D_r^{11} & \ldots & D_r^{1p} & G_r^{11} & \ldots & G_r^{1n} & 0 & \ldots & 0 \\
\vdots & \ddots & \vdots & \vdots & \ddots & \vdots & \vdots & \ddots & \vdots & \vdots & \ddots & \vdots \\
0 & \ldots & 0 & D_r^{(m-n)1} & \ldots & D_r^{(m-n)p} & G_r^{(m-n)1} & \ldots & G_r^{(m-n)n} & 0 & \ldots & 0
\end{bmatrix} \tag{11}
$$

where $\mathbf{Y} = \mathbf{G}_s^{-1}$ and $\mathbf{X} = -\mathbf{G}_s^{-1}\mathbf{D}_s$. Note that, X^{ij} represents the ijth component in the matrix $\mathbf{X}$. Furthermore, Eq. (11) can be rewritten in the block-matrix form displayed in Eq. (12),

$$\mathbf{A}_w^{cl} = \begin{bmatrix} \mathbf{0} & \mathbf{0} & \mathbf{Y}' & \mathbf{0} \\ \mathbf{0} & \mathbf{0} & \mathbf{X}' & \mathbf{D}_r' \\ \mathbf{Y} & \mathbf{X} & \mathbf{0} & \mathbf{G}_r' \\ \mathbf{0} & \mathbf{D}_r & \mathbf{G}_r & \mathbf{0} \end{bmatrix} \qquad (12)$$

where the four columns/rows represent the vertices $\left[\mathbf{y}_s^{sp}\,\mathbf{d}\,\mathbf{u}\,\mathbf{y}_r\right]$, respectively. This adjacency matrix parameterizes all the potential control structures for any selection of $\mathbf{G}_s$, i.e. the weighted graph topology is the same.

Since the adjacency matrix $\mathbf{A}_w^{cl}$ has information about the control policy and the allowed (structural) interaction between vertices, it can be used to evaluate the incidence between vertices in a SSD sense. Indeed, if each vertex is analyzed as an independent variable the effect of its changes among all the vertices can be stated as a function of the graph structure. Let us consider the set

$$V = \{\mathbf{y}_s^{sp}, \mathbf{d}, \mathbf{u}, \mathbf{y}_r\}$$
$$= \{y_{s1}^{sp}, \ldots, y_{sn}^{sp}, d_1, \ldots, d_p, u_1, \ldots, u_n, y_r^1, \ldots, y_r^{m-n}\} \qquad (13)$$

which groups together all the vertices of the weighted graph, then the SSD index can be stated as

$$\text{SSD}(V) = \sum_{i=1}^{m+n+p} ||\mathbf{A}_w^{cl}\mathbf{e}(i)||_2^2 = ||\mathbf{A}_w^{cl}(:,1)||_2^2 + \cdots$$
$$+ ||\mathbf{A}_w^{cl}(:,m+n+p)||_2^2 = ||\mathbf{A}_w^{cl}||_F^2 = 2[\text{tr}(\mathbf{YY}') + \text{tr}(\mathbf{XX}')$$
$$+ \text{tr}(\mathbf{D}_r\mathbf{D}_r') + \text{tr}(\mathbf{G}_r\mathbf{G}_r')] = 2(||\mathbf{Y}||_F^2 + ||\mathbf{X}||_F^2 + ||\mathbf{D}_r||_F^2$$
$$+ ||\mathbf{G}_r||_F^2) = 2\sum_{i=1}^{2n+p} ||\mathbf{A}_w^{cl*}\mathbf{e}^*(i)||_2^2 = 2||\mathbf{A}_w^{cl*}||_F^2 \qquad (14)$$

where $\mathbf{A}_w^{cl*}$ is a particular block selection (lower-left corner) of the original $\mathbf{A}_w^{cl}$ matrix given by,

$$\mathbf{A}_w^{cl*} = \begin{bmatrix} \mathbf{Y} & \mathbf{X} & \mathbf{0} \\ \mathbf{0} & \mathbf{D}_r & \mathbf{G}_r \end{bmatrix} \qquad (15)$$

and the vectors $\mathbf{e}(i)$ and $\mathbf{e}^*(i)$ have $(m+n+p)$ and $(2n+p)$ components, respectively, an unitary entry in the ith location and zero elsewhere.

From Eq. (14) can be observed that the SSD index applied to all vertices in the weighted graph ($\mathbf{A}_w^{cl}$) is reduced to the effects found in the $\mathbf{u}$ and $\mathbf{y}_r$ vector vertices due to changes in the $\mathbf{y}_s^{sp}$, $\mathbf{d}$, and $\mathbf{u}$ ones ($\mathbf{A}_w^{cl*}$). This result is not surprising because of the chosed closed-loop structure and the symmetric properties of the adjacency matrix $\mathbf{A}_w^{cl}$. In other words, the deviations in all vertices can be quantified via the deviations on the MVs and UVs vertices only.

This last statement indicates the strong resemblances between the SSD($\mathbf{y}_r$) approach shown in Eq. (4) and the current SSD(V) methodology based on the weighted graph. In fact, if the relationship in Eq. (14) is analyzed by using the norm and singular value expressions displayed in Eq. (6), the following inequality can be obtained,

$$\frac{1 + \underline{\sigma}(\mathbf{D}_s) + \underline{\sigma}(\mathbf{G}_s)\left[\overline{\sigma}(\mathbf{D}_r) + \overline{\sigma}(\mathbf{G}_r)\right]}{\underline{\sigma}(\mathbf{G}_s)} \leq ||\mathbf{A}_w^{cl}||_F = \sqrt{2}||\mathbf{A}_w^{cl*}||_F \qquad (16)$$

From a control perspective, minimizing $||\mathbf{A}_w^{cl}||_F$ implies that MVs and UVs deviations are explicitly minimized under the multivariate effects introduced by $\mathbf{y}_s^{sp}$, $\mathbf{d}$ and $\mathbf{u}$ deviations. Note that in the SSD($\mathbf{y}_r$) case the MVs deviations are quantified implicitly. On
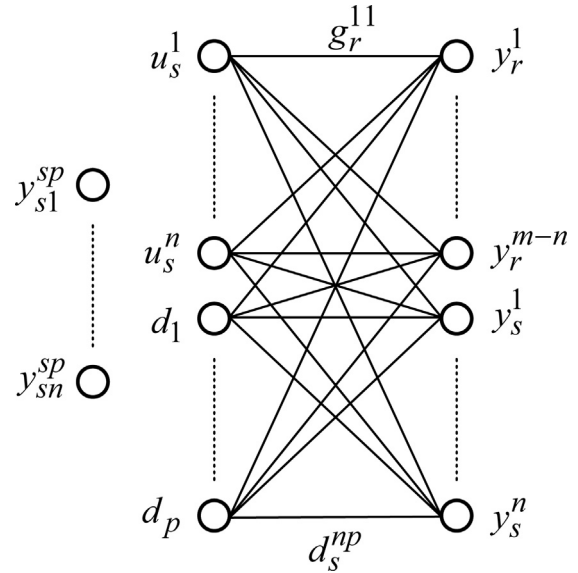

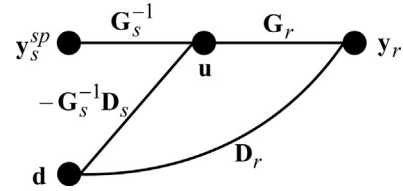**Fig. 2.** Weighted graph G_{ol} – open-loop process.

Fig. 3. Weighted graph G_{cl} – closed-loop process.

the other hand, Eq. (16) shows that the main source of singularity in this expression is the minimum singular value $\underline{\sigma}(\mathbf{G}_s)$. Hence, the minimization of $||\mathbf{A}_w^{cl}||_F$ additionally tends to increase $\underline{\sigma}(\mathbf{G}_s)$ in a trade-off solution. This is an important characteristic, as mentioned in Section 2.1, because it gives some insights about the system to be controlled.

Furthermore, remembering the singular energy definition for weighted graphs given in Eq. (10), the Schatten p-norms definition given in Bhatia (1996) and Zhan (2002), and the adjacency matrix in Eq. (12), we have

$$||\mathbf{A}_w^{cl}||_p = \left[\sum_{i=1}^r \sigma_i^p(\mathbf{A}_w^{cl})\right]^{1/p}, \qquad p \geq 1 \qquad (17)$$

it is clear that $\mathbb{E}_s(G_{cl}) = ||\mathbf{A}_w^{cl}||_1$ is the well-known "nuclear norm" or "trace norm". Some classical norms can be derived from the Schatten p-norms, i.e. the Frobenius norm $||\mathbf{A}||_2 = ||\mathbf{A}||_F$ and the spectral norm $||\mathbf{A}||_\infty$, for any matrix $\mathbf{A}$.

In this context, from the symmetric norms theory in Bhatia (1996), the following inequality can be stated

$$||\mathbf{A}_w^{cl}||_\infty \leq ||\mathbf{A}_w^{cl}||_* \leq ||\mathbf{A}_w^{cl}||_1 \qquad (18)$$

for all unitarily invariant norms $||\mathbf{A}_w^{cl}||_*$. The Frobenius norm fulfills the last condition, hence the relationship between the SSD-based deviations in Eq. (16) and the singular energy of the weighted graph can be stated as shown in Eq. (19),

$$\frac{1 + \underline{\sigma}(\mathbf{D}_s) + \underline{\sigma}(\mathbf{G}_s)\left[\overline{\sigma}(\mathbf{D}_r) + \overline{\sigma}(\mathbf{G}_r)\right]}{\underline{\sigma}(\mathbf{G}_s)} \leq ||\mathbf{A}_w^{cl}||_F \leq \mathbb{E}_s(G_{cl}) \qquad (19)$$

The inequality in Eq. (19) shows that the singular energy, $\mathbb{E}_s(G_{cl})$, of the weighted graph structure displayed in Fig. 3 is the upper bound of the SSD index based on its weighted adjacency matrix

$\mathbf{A}_w^{cl}$. In other words, the singular energy of the closed-loop weighted graph, $\mathbb{E}_s(G_{cl})$, is also a quantification of the MVs and UVs deviations with the properties discussed previously. Indeed, the minimization of $\mathbb{E}_s(G_{cl})$ produces the minimization of $||\mathbf{A}_w^{cl}||_F$, therefore the PWC problem addressed here can be stated as a singular-energy-based approach with similar characteristics to the sum SSD one.

Remark 1: $\mathbb{E}_s(G_{cl})$ is defined as the sum of the singular values computed from the weighted adjacency matrix (see the nuclear norm in Eq. (10)). Considering Eqs. (14), (15) and (18), and the multivariable gain concepts ($\underline{\sigma}(\mathbf{A}) \leq$ multivariable gain of $\mathbf{A} \leq \overline{\sigma}(\mathbf{A})$) it is clear that this singular energy has information of the multivariable gain from $\{\mathbf{y}_s^{sp}, \mathbf{d}, \mathbf{u}\}$ to $\{\mathbf{y}_r, \mathbf{u}\}$. In other words, if the singular energy is low, then, the deviation in $\{\mathbf{y}_r, \mathbf{u}\}$ will also be low for most disturbance directions in $\{\mathbf{y}_s^{sp}, \mathbf{d}, \mathbf{u}\}$ (i.e. low multivariable gain). So, for the proposed graph, the singular energy is directly related to deviations on $\{\mathbf{y}_r, \mathbf{u}\}$, i.e. uncontrolled variables and manipulated variables. This concept is very helpful from the point of view of process and control engineers. Also helpful is the graphical representation of the weighted graph which allows to quickly identify and evaluate process variables (vertices) interactions.

If a suitable parametrization is selected for the process partitioning in Eq. (1) and the IMC control structure is considered for the weighted graph construction in Fig. 3, the optimal CVs selection can be performed by

$$\min_{\mathbf{G}_s} \mathbb{E}_s(G_{cl}), \quad \text{subject to } \det(\mathbf{G}_s) \neq 0 \qquad (20)$$

where the condition $\det(\mathbf{G}_s) \neq 0$ guarantees the feasibility of the future IMC structure. Again here, the combinatorial problem stated in Eq. (20) can be efficiently solved via exhaustive search or some mixed-integer optimization routine depending on the process dimension.

Remark 2: Although SSD($\mathbf{y}_r$)-based and $\mathbb{E}_s(G_{cl})$-based methodologies have similar global properties and similar physical interpretations, the deep analysis shown in this paper displays clear differences regarding the evaluated deviations. The SSD($\mathbf{y}_r$) methodology minimizes the deviations in $\mathbf{y}_r$ based on the law stated in Eq. (3) by accounting $\mathbf{S}_{sp}$ and $\mathbf{S}_d$. In this context, the deviations in the manipulated variables, $\mathbf{u}$, are minimized implicitly (Eq. (7)). On the other hand, the $\mathbb{E}_s(G_{cl})$-based approach quantifies directly the SSD(V) from Eq. (16), and if we consider Eq. (15), it is clear that this singular energy measures the deviations in $\mathbf{y}_r$ and $\mathbf{u}$ explicitly. These differences can also be observed and commented in the next section.

4. Case study: Shell oil fractionator

The Shell heavy oil fractionator process (Maciejowski, 2002; Zumoffen & Basualdo, 2013) is considered here for testing the optimal CVs selection procedures commented in previous sections. The plant is a distillation column with a gaseous feed entering at the fractionator bottom.

The overall process layout can be observed in Fig. 4 and its approximated model is shown in Table 1. The involved variables have the following description: y_1 – the top end point composition, y_2 – the side end point composition, y_3 – the top temperature, y_4 – the upper reflux temperature, y_5 – the side draw temperature, y_6 – the intermediate reflux temperature, y_7 – the bottoms reflux temperature, u_1 – the top draw flow, u_2 – the side draw flow, u_3
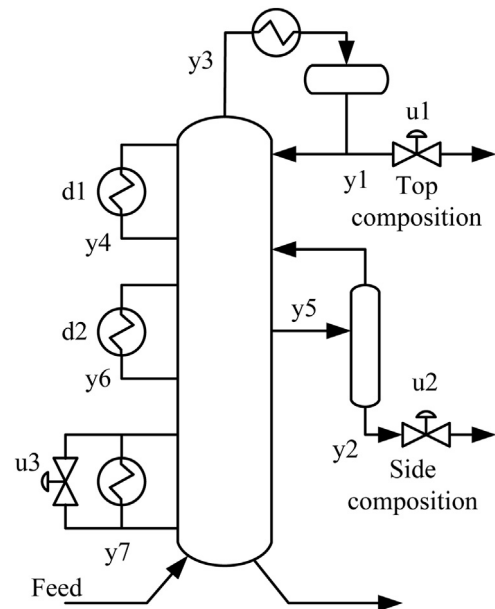

Fig. 4. Shell oil fractionator process.

Table 1
Shell oil fractionator model.

	$\mathbf{G}(s)$			$\mathbf{D}(s)$	
	u_1	u_2	u_3	d_1	d_2
y_1	$\frac{4.05e^{-27s}}{50s+1}$	$\frac{1.77e^{-28s}}{60s+1}$	$\frac{5.88e^{-27s}}{50s+1}$	$\frac{1.20e^{-27s}}{45s+1}$	$\frac{1.44e^{-27s}}{40s+1}$
y_2	$\frac{5.39e^{-18s}}{50s+1}$	$\frac{5.72e^{-14s}}{60s+1}$	$\frac{6.90e^{-15s}}{40s+1}$	$\frac{1.52e^{-15s}}{25s+1}$	$\frac{1.83e^{-15s}}{20s+1}$
y_3	$\frac{3.66e^{-2s}}{9s+1}$	$\frac{1.65e^{-20s}}{30s+1}$	$\frac{5.53e^{-2s}}{40s+1}$	$\frac{1.16}{11s+1}$	$\frac{1.27}{6s+1}$
y_4	$\frac{5.92e^{-11s}}{12s+1}$	$\frac{2.54e^{-12s}}{27s+1}$	$\frac{8.10e^{-2s}}{20s+1}$	$\frac{1.73}{5s+1}$	$\frac{1.79}{19s+1}$
y_5	$\frac{4.13e^{-5s}}{8s+1}$	$\frac{2.38e^{-7s}}{19s+1}$	$\frac{6.23e^{-2s}}{10s+1}$	$\frac{1.31}{2s+1}$	$\frac{1.26}{22s+1}$
y_6	$\frac{4.06e^{-8s}}{13s+1}$	$\frac{4.18e^{-4s}}{33s+1}$	$\frac{6.53e^{-s}}{9s+1}$	$\frac{1.19}{19s+1}$	$\frac{1.17}{24s+1}$
y_7	$\frac{4.38e^{-20s}}{33s+1}$	$\frac{4.42e^{-22s}}{44s+1}$	$\frac{7.20}{19s+1}$	$\frac{1.14}{27s+1}$	$\frac{1.26}{32s+1}$

– the bottoms reflux duty, d_1 – the intermediate reflux duty, and d_2 – the upper reflux duty. The main objective of the plant is producing top and side draw products with specific qualities. In this context, the Shell oil fractionator represents a PWC problem with $m = 7$ potential CVs, $n = 3$ available MVs, and $p = 2$ DVs.

In this context, the optimal CVs selection approaches based on SSD($\mathbf{y}_r$) and $\mathbb{E}_s(G_{cl})$ are applied here for sake of comparison. This problem present $m!/n!(m-n)! = 7!/(3!(7-3)!) = 35$ potential solutions, so it can be easily solved via exhaustive search.

Fig. 5 summarizes the most important matrix properties for $\mathbf{G}_s$ involved in both minimizations. Note that in all figures the potential solutions are ordered from the best (no. 1) to the worst (no. 35) case by using its corresponding functional cost. Indeed, Fig. 5a and b displays the minimum and maximum singular value evolutions $\underline{\sigma}(\mathbf{G}_s)$ and $\overline{\sigma}(\mathbf{G}_s)$ (or $\sigma_{min}(\mathbf{G}_s)$ and $\sigma_{max}(\mathbf{G}_s)$), respectively. It is clear that the SSD-based and the Es-based methodologies have similar results from these matrix properties point of view, i.e. the search is always guided towards well-conditioned optimal solutions. The latter means that the selected subprocess to be controlled, $\mathbf{G}_s$, minimizes both the multivariable SSD gain/singular energy and the condition number.

Fig. 6 shows the evolution of the functional costs (in logarithmic scales) for all the solutions. Fig. 6a summarizes the $\mathbb{E}_s(G_{cl})$ index profile and its comparison with the Frobenius norm from Eq. (19), thus depicting the upper bound conditions. Furthermore, for sake
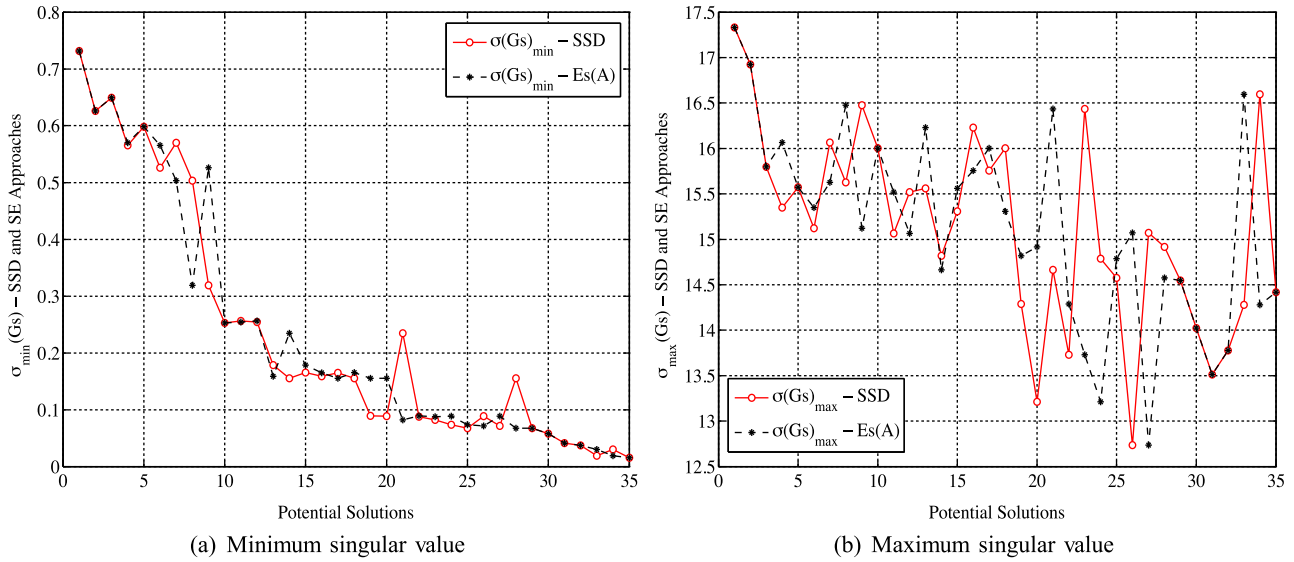
Fig. 5. (a and b) Singular values of $\mathbf{G}_s$ – SSD($\mathbf{y}_r$) and $\mathbb{E}_s(G_{cl})$.
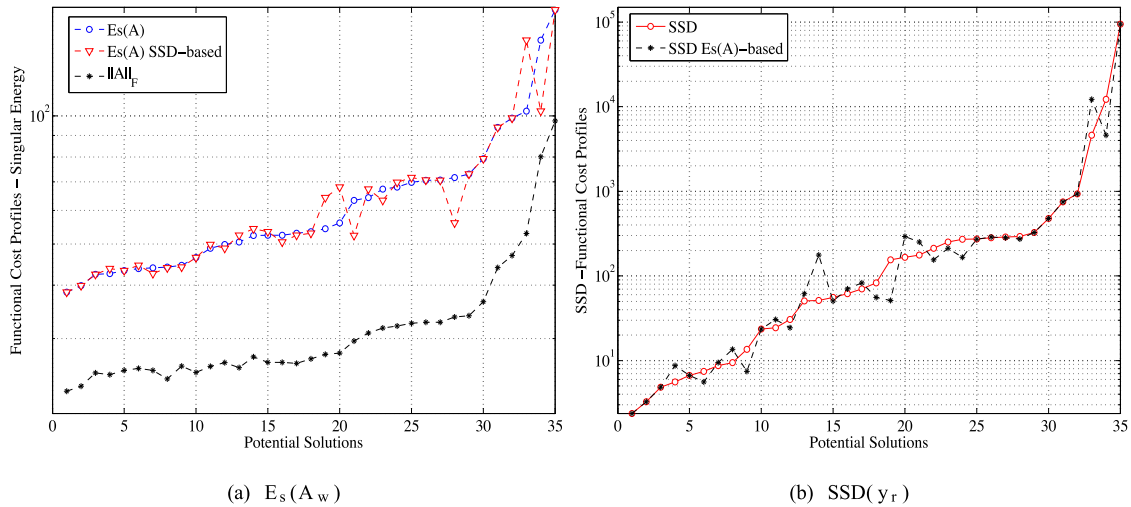

Fig. 6. (a and b) Functional costs.

of comparison, we compute the singular energy for the solutions suggested by the SSD($\mathbf{y}_r$) index, and call it "$\mathbb{E}_s(G_{cl})$ SSD-based". Similarly, Fig. 6b shows the profile of the SSD($\mathbf{y}_r$) index in contrast with the sum of square deviations computed on the solutions suggested by the $\mathbb{E}_s(G_{cl})$ approach (this index is called "SSD $\mathbb{E}_s(G_{cl})$-based"). From Fig. 6a and b it is evident that the minimization of the sum of square deviations for the UVs, SSD($\mathbf{y}_r$), has very similar effects than the minimization proposed via the singular weighted graph energy, $\mathbb{E}_s(G_{cl})$.

The best five solutions given by each methodology are listed in Table 2 with their corresponding SSD($\mathbf{y}_r$) and $\mathbb{E}_s(G_{cl})$ indexes. According to this table, the only different CV selection is the suggested by solution number 4; the remainder solutions are the same for both methodologies. It is important to note that the overall search performed in Eq. (5) as well as Eq. (20) were made without considering the original control requisites, i.e. a free search was performed. These requisites can be considered once the optimization problem was solved by selecting the suitable solution from Table 2. Indeed, if the original control requisites stated by Maciejowski (2002) are taken into account (i.e. it is important to ensure the products quality (y_1 and y_2)), the best solution to this

problem is the number 3, which selects y_1 (top composition), y_2 (side composition) and y_7 (bottom temperature), marked with (*) in the corresponding table. As a consequence, both the control requisites and the SSD/Energy minimization are fulfilled.

Further developments based on $\mathbb{E}_s(G_{cl})$ could incorporate some weighted effects on the searching procedure as suggested in Zumoffen and Basualdo (2013) for the SSD($\mathbf{y}_r$) approach. This weighted search considers the original control requisites as well as the relative degree of importance between variables explicitly on the functional cost. The dynamic evaluation of solution number 3, at closed loop, is not presented here because it is extensively analyzed in Zumoffen and Basualdo (2013).

Fig. 7 compares the inequalities presented in Eqs. (7) and (19) for this case study. Both sides of these inequalities are analyzed, with particular emphasis on the partial contributions involved in each left-hand side. Fig. 7a displays the majorization given by SSD($\mathbf{y}_r$) to some minimum and maximum singular values of the process submatrices along the solutions. It is clear that this inequality holds and due to the implicitly relationship between $\mathbf{y}_r$ and $\mathbf{u}$ both contributions called $\underline{\sigma}(\mathbf{G}_r)/\underline{\sigma}(\mathbf{G}_s)$ and $|\overline{\sigma}(\mathbf{D}_r) - \overline{\sigma}(\mathbf{G}_r\mathbf{G}_s^{-1}\mathbf{D}_s)|$ are intended to be minimized. This shows that, even though SSD($\mathbf{y}_r$) aims to

Table 2
Best first five solutions – Shell process.

No.	CVs selected							SSD($\mathbf{y}_r$)	CVs selected							$\mathbb{E}_s(G_{cl})$
	y_1	y_2	y_3	y_4	y_5	y_6	y_7		y_1	y_2	y_3	y_4	y_5	y_6	y_7	
1	0	1	0	1	0	0	1	2.37	0	1	0	1	0	0	1	38.55
2	0	1	0	1	0	1	0	3.26	0	1	0	1	0	1	0	39.92
3*	1	1	0	0	0	0	1	4.83	1	1	0	0	0	0	1	42.43
4	1	1	0	0	0	1	0	5.59	0	1	0	0	1	0	1	42.62
5	0	1	1	0	0	0	1	6.68	0	1	1	0	0	0	1	43.27

(a) SSD($\mathbf{y}_r$)-based approach

(b) $E_s(G_{cl})$-based approach
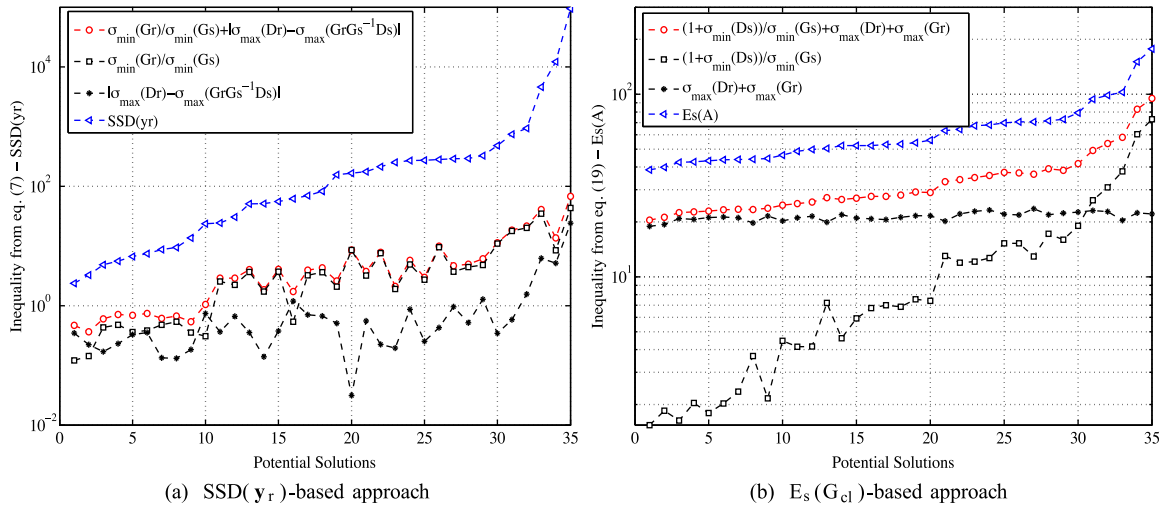
Fig. 7. (a and b) Evaluating Eqs. (7) and (19).

(a) Solution no. 3 - Optimal selected here

(b) Solution no. 17 - Intermediate solution

(c) Solution no. 35 - Worst solution
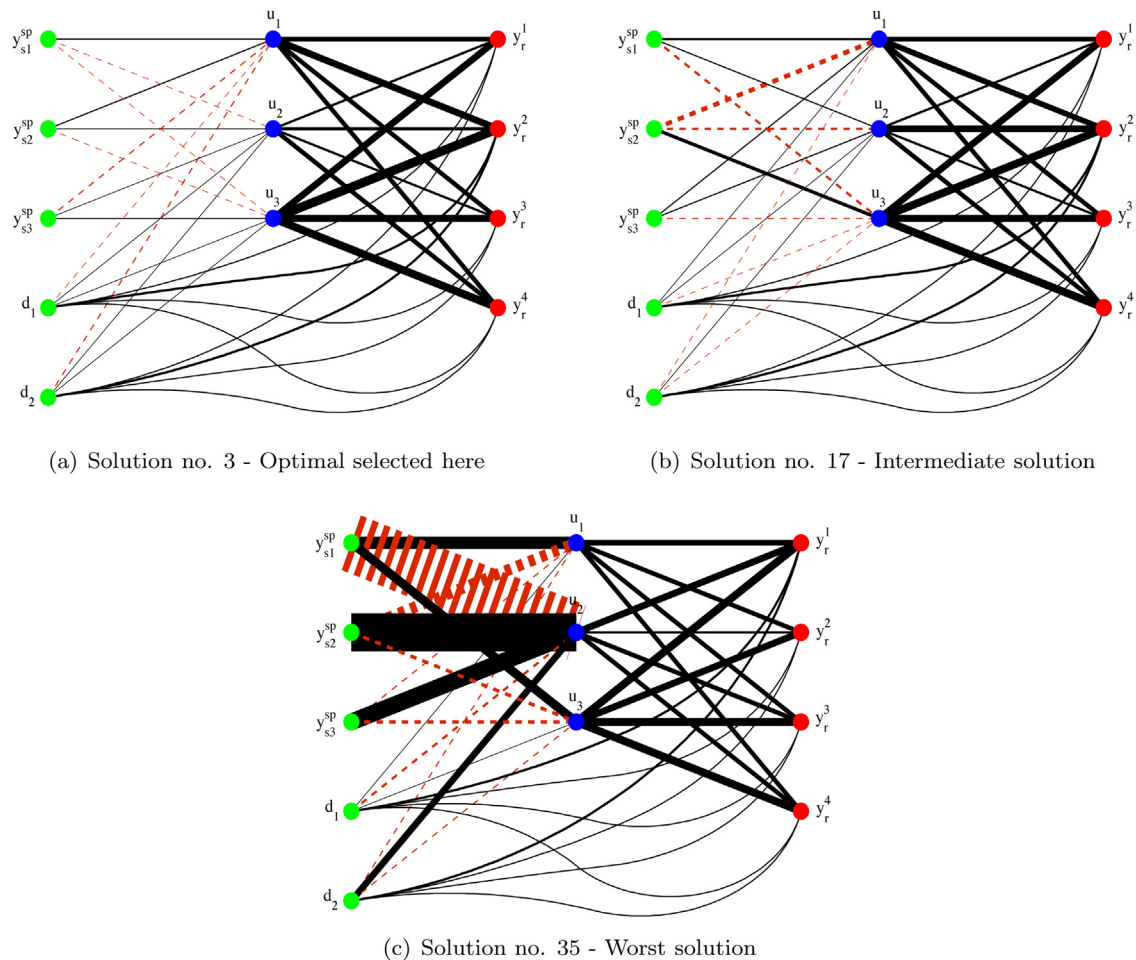
Fig. 8. (a–c) Evolution of the weighted graph with $\mathbb{E}_s(G_{cl})$. (For interpretation of color in the text, the reader is referred to the web version of the article.)

increase $\underline{\sigma}(\mathbf{G}_s)$ this improvement has a negative influence on the latter component with absolute value, thus presenting a trade-off. Fig. 7b summarizes the majorization profiles given by $\mathbb{E}_s(G_{cl})$ in Eq. (19). Although the singular energy minimization also reduces the UVs and MVs deviations in a SSD sense, the situation here is a bit different (as discussed in Section 3, Remark 2). In fact, the $(1 + \underline{\sigma}(\mathbf{D}_s))/\underline{\sigma}(\mathbf{G}_s)$ component is mainly minimized by increasing the minimum singular value $\underline{\sigma}(\mathbf{G}_s)$ since the multivariate gain of $[\overline{\sigma}(\mathbf{D}_r) + \overline{\sigma}(\mathbf{G}_r)]$ is reduced more smoothly.

Finally, we present in Fig. 8 a graphical visualization for this optimal CVs selection, based on the graphs adjacency matrix $\mathbf{A}_w^{cl}$. The weighted graph structure displayed in Fig. 3, for the process at closed loop and perfect control, is shown here for three different graph instances. Fig. 8a, b, and c shows the weighted graphs for solutions number 3 (optimal selected here), 17 (intermediate), and 35 (worst), respectively. Note that, for improving visualization, black-continuous-weighted lines are used for positive gains, and red-dashed-weighted lines represent negative ones. These graphs make evident that the $\mathbb{E}_s(G_{cl})$-based CVs selection leads to select $\mathbf{G}_s$ such that a balanced interaction between vertices is achieved. Indeed, remembering that the relationships between the vector vertices "$\mathbf{y}_s^{sp} - \mathbf{u}$" and "$\mathbf{d} - \mathbf{u}$", are given by $\mathbf{G}_s^{-1}$ and $-\mathbf{G}_s^{-1}\mathbf{D}_s$, respectively, then, those solutions which minimize the singular energy will produce weighted graph structures with minimum interaction between these vertices. This fact is clear from Fig. 8c where the worst solution is displayed indicating heavy interactions between "set points-MVs" and "DVs-MVs" vector vertices. It is important to highlight the importance of the closed-loop representation given in Fig. 8 as a tool for quickly identifying the magnitude and direction of influences between process variables at steady state. Moreover, when the process dimension tends to deteriorate the graphical visualization, due to a large number of vertices and edges, the graph in Fig. 8 can be changed by the matrix-based representation suggested in Fig. 3, but weighting the vector edges with the absolute sum of individual edges.

5. Conclusions and future work

In this work a new perspective for solving the optimal controlled variables (CVs) selection problem (a PWC subproblem) was successfully presented. The methodology is based on the graph theory which allows to represent many real-word situations conveniently, whether from the graphical as well as mathematical point of views. Indeed, the optimal CVs selection is based on the singular energy of weighted graphs. It was found that if the closed-loop process (at steady state and perfect control) is represented by a weighted graph, its energy (based on its adjacency matrix) is strongly (and explicitly) related to deviations in manipulated and uncontrolled variables of the plant. Moreover, this work shows that the singular energy is the upper bound (majorizes) of the interaction effects in all the vertices of the weighted graph in a sum of square deviation (SSD) sense (Frobenius norm). Explicitly, the SSD concept applied to the overall graph structure is reduced to quantify the deviations in the manipulated variables and uncontrolled variables vertices only. This result shows clear structural resemblances with the approach called SSD presented by Molina et al. (2011) and Zumoffen and Basualdo (2013), but in this case from a spectral graph theory standpoint. Hence, the optimal CVs selection can be performed by minimizing the singular energy of the graph. Furthermore, the analysis proposed in this work shows that this minimization has similar properties to those presented by the SSD one. Particularly, both methodologies tend to improve the matrix conditioning of the subprocess to be controlled, i.e. tend to maximize its minimum singular value. The latter is an

important quality strongly related to the final closed-loop behavior. Finally, the graph closed-loop visualization was presented and described as a very helpful tool for quickly identifying the magnitude and direction of influences between process variables at steady state. These facts help the designers to perceive the complexity of the processes and their corresponding control problems. Future work will be related to the analysis of the presented graphs using the powerful tools made available by the spectral graph theory.

References

Bhatia, R. (1996). *Matrix analysis. No. 169 in Graduate texts in mathematics*. Springer-Verlag.

Bondy, J., & Murty, S. (1985). *Graph theory with applications* (5th ed., pp.). Elsevier Science Publishing Co., Inc.

Castaño Arranz, M., & Birk, W. (2012). New methods for interaction analysis of complex process using weighted graphs. *Journal of Process Control, 22*, 280–295.

Cvetković, D., Rowlinson, P., & Simić, S. (2010). *An introduction to the theory of graph spectra. No. 75 in London Mathematical Society*. Cambridge University Press.

Cvetković, D., & Simić, S. (2011). Graph spectra in computer science. *Linear Algebra and its Applications, 434*, 1545–1562.

Garcia, C., & Morari, M. (1985). Internal model control. 2. Design procedure for multivariable systems. *Industrial & Engineering Chemistry Process Design and Development, 24*, 472–484.

Golub, G., & Loan, C. V. (1996). *Matrix computations* (3rd ed., pp.). Johns Hopkins University Press.

Grosdidier, P., Morari, M., & Holt, B. (1985). Closed-loop properties from steady-state gain information. *Industrial & Engineering Chemistry Fundamentals, 24*, 221–235.

Gutierrez-Perez, J., Herrera, M., Perez-Garcia, R., & Ramos-Martinez, E. (2011). Application of graph-spectral methods in the vulnerability assessment of water supply networks. *Mathematical and Computer Modelling*, http://dx.doi.org/10.1016/j.mcm.2011.12.008

Gutman, I. (2005). Topology and stability of conjugated hydrocarbons. the dependence of total pi-electron energy on molecular topology. *Journal of Serbian Chemical Society*, 441–456.

Gutman, I., Li, X., & Zhang, J. (2009). Analysis of complex networks. From biology to linguistics. In *Graph energy*. Wiley-VCH.

Gutman, I., & Shao, J. (2011). The energy change of weighted graphs. *Linear Algebra and its Applications, 435*, 2425–2431.

Horn, R., & Johnson, C. (1990). *Matrix analysis*. Cambridge University Press.

Khaki-Sedigh, A., & Moaveni, B. (2009). *Control configuration selection for multivariable plants*. Springer-Verlag Berlin Heidelberg.

Maciejowski, J. (2002). *Predictive control with constraints*. Prentice Hall.

Molina, G., Zumoffen, D., & Basualdo, M. (2011). Plant-wide control strategy applied to the Tennessee Eastman process at two operating points. *Computers & Chemical Engineering, 35*, 2081–2097.

Nikiforov, V. (2007). The energy of graphs and matrices. *Journal of Mathematical Analysis and Applications, 326*, 1472–1475.

Skogestad, S., & Postlethwaite, I. (2005). *Multivariable feedback control. Analysis and design* (2nd ed., pp.). John Wiley & Sons.

Skogetad, S., & Morari, M. (1987). Implications of large RGA elements on control performance. *Industrial & Engineering Chemistry Research, 26*, 2323–2330.

Yang, F., Shah, S., & Xiao, D. (2012). Signed directed graph based modeling and its validation from process knowledge and process data. *International Journal of Applied Mathematics and computer Science, 22*, 41–53.

Zhan, X. (2002). *Matrix inequalities. No. 1790 in Lecture notes in mathematics*. Springer-Verlag.

Zumoffen, D., & Basualdo, M. (2010). A systematic approach for the design of optimal monitoring systems for large scale processes. *Industrial & Engineering Chemistry Research, 49*, 1749–1761.

Zumoffen, D., & Basualdo, M. (2012). Avoiding oversizing in plant-wide control designs for industrial processes. *Computer Aided Chemical Engineering, 30*, 937–941.

Zumoffen, D., & Basualdo, M. (2013). Improvements on multiloop control design via net load evaluation. *Computers & Chemical Engineering, 50*, 54–70.